iomac
International Operational Modal Analysis Conference

11th International Operational Modal Analysis Conference

20 - 23 May 2025 | Rennes, France

Use of ensemble learning in damage identification based on curvature analysis

Daniele Dessi [1], *and Andrea Venturi* [2], *and Fabio Passacantilli* [1]

[1] National Research Council, Institute of Marine Engineering, Rome, Italy, daiele.dessi@cnr.it
[2] Sapienza University of Rome, Department of structural and geotechnical engineering, Rome, Italy

ABSTRACT
The analysis and comparison of spatial invariants shaping the structural system response is the basis of several damage identification methods, such as those employing mode shape analysis. Approaches based on strain energy assume that damage-induced changes in physical properties are more detectable if curvatures are considered. The application of physics-based techniques requiring a baseline typically provides an index distribution over the considered structure which detects local damage depending on exceeding a certain threshold (damage condition). This threshold is typically decided by setting the confidence level in assessing the damage, a key parameter for data affected by uncertainties which tunes the balance of false positives and false negatives. To increase the accuracy of the positive predictions without significantly compromising the sensitivity, an alternative is provided by the definition of a macro-index (Dessi *et al.* [1]), which is a combination of different indices based on an ensemble learning principle. Here, four different indices are applied to experimentally identify a local reduction in the thickness of a hollow beam. It is shown that damage identification results are improved if ensemble learning is employed. Thus, different voting schemes are used for the definition of the macro-index, resulting in a comparison of their effectiveness in terms of identification accuracy.

Keywords: Damage detection, Modal analysis, Experimental testing, Ensemble learning

1. INTRODUCTION

Damage identification methods based on analyzing dynamical response benefit from comparing response invariants extracted in reference and potentially damaged conditions. A popular approach is considering modal curvature variation, as it relates to stiffness changes. Many methods have been developed over the last three decades, starting with Pandey *et al.* [2]. Most of these methods can be derived from Fan and Qiao's general formulation [3], as demonstrated in Dessi and Camerlengo [4], where they were applied

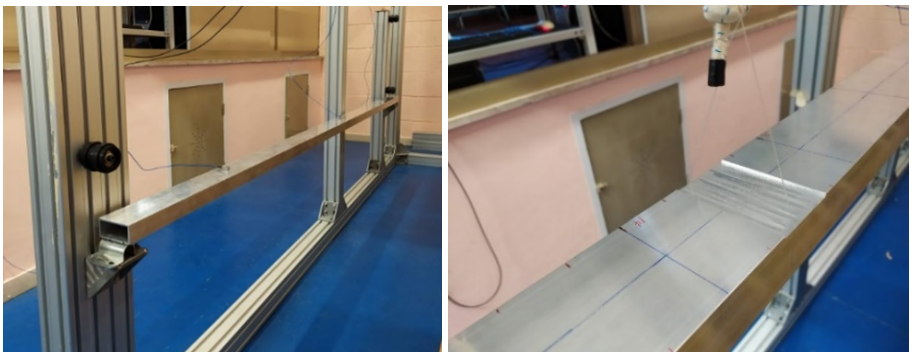

(a) Beam simply supported at the ends. (b) Detail of thickness reduction of the beam top side.

Figure 1: Experimental set-up in the LabSDD at CNR-INM.

and compared on analytically calculated modal parameters. In Dessi *et al.* [1], the comparison was extended to a real case, a slender beam under different boundary conditions (BCs), addressing several sources of experimental uncertainties in both damage localization and severity estimation. These uncertainties were mitigated by introducing a macro-damage index. In the present study, we focus on the use of ensemble learning upon which the macro-index is defined, a key feature that has not been fully clarified in the previous paper. We propose and compare different voting schemes as alternatives to the full agreement condition previously employed. Results show that ensemble learning can effectively predict damage more reliably with respect to the separate evaluation of the damage indices.

2. CONSIDERED DAMAGE AND EXPERIMENTAL SET-UP

The structure generating the experimental data is a hollow aluminum beam with a rectangular hollow section, whose characteristics are listed in Table 1.

Table 1: Geometrical and physical characteristics of the intact beam.

Length	Width	Height	Thickness	Young modulus	Density
$2.918\,\mathrm{m}$	$0.080\,\mathrm{m}$	$0.040\,\mathrm{m}$	$0.004\,\mathrm{m}$	$67 \cdot 10^9\,\mathrm{Pa}$	$2.677\,\mathrm{Kg/m^3}$

The beam was properly constrained at the edges to produce simply supported (SS) BCs as shown in Figs. 1(a) and 1(b). In [5] the vibration modes of the beam excited with random impacts by tapping the upper surface with a pencil were identified using OMA, which processed $N_{exp} = 9$ mono-axial accelerometers PCB333B32 equally spaced along the beam. In the present study, the roving hammer technique (RHT) was used to increase the spatial resolution ($N_{exp} = 19$). The authors proved that OMA provides less noisy modes than those that can be obtained by RHT with the same test duration. The use of RHT, along with the repeated application of imperfect SS BCs each time the beam is structurally modified, makes the present experimental data more noise-sensitive than those obtained from OMA over soft-spring mounted beam in [5]. The stiffness reduction was locally obtained by progressively reducing the thickness of the sides of the section. The damage was introduced at two different positions: in the middle of element E_{04} and in the middle of element E_{14} (element E_j are numbered from left to right). Thinning was performed in several stages by milling to obtain different beam sectional stiffnesses corresponding to distinct damage levels, as shown in Table 2. The length of the damage is one third of the distance between two experimental nodes, about $0.05\,\mathrm{m}$. The sensor signals were acquired using the LMS SCADAS SCM05 acquisition system with 24 VB8 channels using Siemens LMS Test.Lab 19 software. Owing to the use of finite differences in the acceleration signals, modal curvatures are available only at the inner points $N_{exp} - 2 = 17$ of the sensor grid. This implies that the modal strain energy or curvature integrals can be calculated only for $N_e = N_{exp} - 3 = 16$ elements. For this reason, the displacement and curvature

Table 2: Intact and damaged beam layouts.

Damage case	$\bar{x}_{14}$	Thinned faces	Local Stiffness ratio	Mean Stiff. ratio in E_{14}	$\bar{x}_{04}$	Thinned faces	Mean Stiff. ratio in E_{04}
R0		0	1	1	N/A	0	1
A1	1.985 m	1	0.721	0.907	N/A	0	1
A2	1.985 m	4	0.43	0.841	N/A	0	1
B1	1.985 m	4	0.43	0.841	0.511 m	1	0.907
B2	1.985 m	4	0.43	0.841	0.511 m	4	0.841

values are recovered at edge points based on ideal BCs, obtaining $N_{exp} = 21$ experimental dofs. Thus, the N_{exp} experimental points divides the beam into $N_e = 20$ elements, indicated as $E_j = [x_j, x_{j+1}]$, where $x_j = j\,h$, and h is the element length.

3. BASELINE METHODS

3.1. Preliminary definitions

The displacement field $w(x,t)$ over the beam can be expressed by modal superposition of the mode shapes $\phi^{(i)}$, with $i = 1, \ldots, M$. Under the hypothesis of small displacements, the beam curvature κ can be also expressed as $\kappa = w''(x,t) = \sum_{i=1}^{M} W^{(i)}(t)\,\kappa^{(i)}(x)$, where $\kappa^{(i)} = \phi^{(i)\prime\prime}(x)$ is the i-th modal curvature ($'$ indicating space derivative), and $W^{(i)}$ is the mode amplitude. Substantially, all the baseline methods compare intact and damage conditions via the use of of modal parameters, such as mode shapes and frequencies. Although the curvatures are more sensitive to damage, they significantly suffer from noisy data, and a direct comparison of intact and damaged curvatures is not straightforward. Thus, integral quantities are usually evaluated, because they do implicitly some kind of spatial average. In the following, several indices, which mostly derive from simplifying the general formulation by Fan and Qiao [3], are briefly presented.

3.2. Damage index definitions

3.2.1. Methods related to strain energy

The modal strain energy is defined as $U^{(i)} = \frac{1}{2}\int_0^L D(x)\,[\kappa^{(i)}(x)]^2\,dx$, with $D(x)$ the sectional bending stiffness, which for element E_j becomes $U_j^{(i)} = \frac{1}{2}\int_{x_j}^{x_{j+1}} D(x)\,[\kappa^{(i)}(x)]^2\,dx$. There exists a value $\bar{D}_j$, relative to the element E_j, such that:

$$U_j^{(i)} = \frac{\bar{D}_j}{2}\int_{x_j}^{x_{j+1}} [\kappa^{(i)}(x)]^2\,dx = \bar{D}_j\,\gamma_j^{(i)}, \tag{1}$$

where $\gamma_j^{(i)}$, being half the integral value, represents a pure geometrical quantity, and similarly for the global strain energy, that is, $U^{(i)} = \bar{D}\,\gamma^{(i)}$. The first two methods related to strain energy are those of Cornwell *et al.* [6] and Stubbs *et al.* [7], which were developed from similar assumptions. Therefore, the Cornwell *et al.* index β_{Co} and for Stubbs *et al.* index β_{St} achieve similar expressions:

$$\beta_{Co} = \frac{\sum_{i=1}^{M}\gamma_j^{(i)}/\gamma^{(i)}}{\sum_{i=1}^{M}\gamma_j^{(i)*}/\gamma^{(i)*}}, \qquad \beta_{St} = \frac{\sum_{i=1}^{M}\gamma^{(i)*}\left(\gamma_j^{(i)} + \gamma^{(i)}\right)}{\sum_{i=1}^{M}\gamma^{(i)}\left(\gamma_j^{(i)*} + \gamma^{(i)*}\right)} \tag{2}$$

where the physical quantities referred to the damaged structure are denoted with *.

Kim and Stubbs [8] proposed a different formulation, by equating the change in system frequencies with the variation of strain energy in the damage element of a uniform beam, leading to the following expression of the stiffness ratio and the damage index:

$$\frac{D_j^*}{\bar{D}} = \frac{\frac{\Delta\lambda_i}{\lambda_i}\gamma^{(i)} + \gamma_j^{(i)}}{\gamma_j^{(i)*}} \rightarrow \beta_{Ki} = \frac{\sum_{i=1}^{M}\left(\frac{\Delta\lambda_i}{\lambda_i}\gamma^{(i)} + \gamma_j^{(i)}\right)}{\sum_{i=1}^{M}\gamma_j^{(i)*}}, \tag{3}$$

where $\lambda_i = \omega_i^2$, $\Delta\lambda_i = \omega_i^2 - \omega_i^{*2}$ and the term depending on the mass variation due to damage at the numerator has been neglected, coherently with the hypothesis that damage produces (mainly) a reduction in the structural stiffness and not in the mass.

3.2.2. Methods related to strain energy

A different family of methods relates the local reduction of stiffness to the comparison of curvature integrals. Choi *et al.* [9] proposed a damage index suitable to be applied to 1D and 2D structures using the concept of compliance under the assumption that the load does not change after damage. They provided the following expression of the index:

$$\beta_{Ch} \simeq \frac{1 + \sum_{i=1}^{M}\int_{x_j}^{x_{j+1}}\left|\kappa^{(i)}(x)\right| dx}{1 + \sum_{i=1}^{M}\int_{x_j}^{x_{j+1}}\left|\kappa^{(i)*}(x)\right| dx} \tag{4}$$

Because all the damage indices introduced above approximate the stiffness ratio D_j^*/D_j, they indicate potential damage if they are less than one.

3.2.3. Index normalization

Owing to the presence of noise in the curvature modes, the damage index is a random variable. It is a common practice for damage localization to introduce a Z-score normalized index, defined as

$$\check{\mathcal{B}}_{\mathrm{idx},j} = \frac{\check{\beta}_{\mathrm{idx},j} - \check{\bar{\beta}}_{\mathrm{idx}}}{\sigma_{\check{\beta}_{\mathrm{idx}}}} \tag{5}$$

where 'idx' refers to a particular index (Cornwell, Stubbs, etc.), $\check{\beta}_{\mathrm{idx},j} = 1/\beta_{\mathrm{idx},j}$ according to the definitions introduced in the previous sections, and $\check{\bar{\beta}}_{\mathrm{idx}}$ and $\sigma_{\check{\beta}_{\mathrm{idx}}}$ are the mean and standard deviation spanning all the beam elements, respectively. In the present study, damage detection (*i.e.*, existence and location) is based on the evaluation of $\check{\mathcal{B}}_{\mathrm{idx},j}$, whereas the assessment of damage severity (*i.e.*, stiffness reduction) is based on $\beta_{\mathrm{idx},j}$.

Therefore, in an ideal error-free condition, positive values of $\check{\mathcal{B}}_{\mathrm{idx},j}$ indicate a possible stiffness reduction, *i.e.*, $D_j^*/D_j < 1$, quantified via the dimensional indices $\beta_{\mathrm{idx},j}$. The choice of the confidence level for the random population $\check{\beta}_{\mathrm{idx}}$ turns into different positive thresholds θ to decide whether an element is damaged ($\check{\mathcal{B}}_{\mathrm{idx},j} \geq \theta$) or not ($\check{\mathcal{B}}_{\mathrm{idx},j} < \theta$). There is no common choice for the threshold, which takes different values depending on the specific application. For instance, the threshold was set to 1 by Park *et al.* [10]), 1.5-1.625 by Choi *et al.* [9] and 2 by Stubbs *et al.* [7].

4. ENSEMBLE LEARNING WITH PHYSICS-BASED METHODS

4.1. Ensemble learning approach

Individual curvature-based methods may exhibit limitations in accuracy and robustness when applied to complex structural conditions. To mitigate these challenges, ensemble learning presents a promising

approach by combining multiple curvature-based damage identification techniques and leveraging their collective decision-making through a voting mechanism. Each technique has strengths and limitations depending on factors such as spatial resolution of mode shapes, boundary conditions and measurement noise. By integrating these methods within an ensemble learning framework, the reliability of damage detection can be spatial resolution of mode shapes enhanced. Though ensemble learning techniques have been specifically introduced for Machine Learning algorithms (see [11] for a review), some concepts can be extended to physics-based models. Each method independently analyse the mode shapes to identify potential damage locations by detecting potential mean curvature anomalies between the experimental nodes. Once the individual assessments are completed, a voting scheme is employed to synthesize their outputs into a collective decision. This voting mechanism can follow different strategies, including unanimity-voting, majority-voting, weighted-voting, or probabilistic fusion, which may be simplified into proportional voting. Unanimity requires full agreement among the methods, while majority voting designates a damage location based on the most frequently identified positions among all methods. In contrast, weighted voting assigns confidence levels to each method based on prior performance or reliability in detecting damage, thereby giving greater influence to more accurate techniques. Probabilistic fusion extends this approach by incorporating statistical models to estimate the likelihood of damage presence at different beam locations.

4.2. Definition of a macro index

The various choices of the damage threshold for the application of individual methods are related to the desired balance between false positives and false negatives that may be targeted. To further mitigate uncertainties, the proposed solution is the definition of a macro index based on the following two-stage process: *i*) an element is potentially classified as damaged or not only according to some agreement scheme (multiple hypothesis testing); *ii*) the average of the (normalized) indices must exceed a given threshold, depending on the confidence level or on more sophisticated reasoning. For instance, in [1] this threshold was set on the basis of Monte Carlo simulations under experimentally identified noise. It is assumed that the generic element E_j is classified as:

- *Damaged,* if it satisfies all the conditions below:
  a) *Agreement conditions*:
    a.1 *Unanimity-voting;* All the normalized index 'positively' agree, *i.e.*, $\forall \mathrm{idx}$, $\check{\mathcal{B}}_{\mathrm{idx},j} > 0$ on the element E_j.
    a.2 *Qualified majority-voting:* All indices except (only) one 'positively' agree, *i.e.*, $\exists! \, \mathrm{idx}$, $\check{\mathcal{B}}_{\mathrm{idx},j} < 0$ on the element E_j.
    a.3 *Proportional-voting:* There is no pre-defined agreement but the decision is based on the strength of each prediction, *i.e.*, the positiveness of the macro-index defined at point b).
  b) *Index-balancing condition*: The average value of the normalized indices, defined as $\bar{\mathcal{B}}_{\mathrm{idx},j} = \sum_{\mathrm{idx}} \check{\mathcal{B}}_{\mathrm{idx},j} > \theta$, with θ a given threshold level θ.
- *Not Damaged,* if does not comply with the assigned condition a), depending on the voting scheme, or does not satisfies condition b).

5. RESULTS

5.1. Simply-supported boundary conditions

5.1.1. Damage existence and location

The experimental noise on the identified mode shapes determine curvature modes rather irregular, as shown in Dessi *et al.* [1], regardless their nature (intact or damaged), even turning positive curvatures into

negative and vice-versa, especially for low order modes. The noise on the curvature modes propagates to the normalized damage indices, introducing both false positives and false negatives, and enhancing the possibility of errors in the damage identification.

In Fig. 2(a), the results relative to the damage localization for damage scenario R0-A1 are reported separately for each of the four indices introduced in Sec. 3.2.. The weighted mean of the stiffness reduction (weights provided by relative intact and damage length inside the element) for element E_{14} is less than $10\,\%$, with a post/pre-damage stiffness ration $D^*_{14}/D_{14} = 0.907$. The value of the normalized index $\check{\mathcal{B}}_{\mathrm{idx},j}$ is reported for each beam element only if it is positive, thus indicating a possible damage. The crossing of a minimum threshold $\theta_{low} = 0.5$, shown as blue bars, determine more reliable predictions (higher confidence), whereas if $\check{\mathcal{B}}_{\mathrm{idx},j} < 0.5$ the bar are colored in cyan. The white bars are relative to the edge elements and suffer from higher uncertainties due to the application of ideal BCs. All the methods identify element E_{14} as damaged, even if Cornwell's index gives a weak score. The methods of Choi and Kim & Stubbs show a smaller number of false positives in different positions. The application of ensemble learning with unanimity-voting (Fig. 2(b)) greatly eliminates most of the false positives introduced, labeling only one element, *i.e.*, E_{19}, as a false positives. It is worth to note that applying qualified majority-voting gives almost same results, with the unique difference of introducing a positive bar on elements E_{13} well below the threshold (not plotted). The same analysis is repeated for a damage-stiffness ratio $D^*_{14}/D_{14} = 0.86$ in Fig.3 corresponding to scenario A1-A2. Cornwell's index and Stubbs' index are more similarly distributed, and show a number of false positives less than those provided by the other indices (see Fig. 3(a)). In Fig. 3(b), the unanimity-voting is first provided by first excluding the Kim & Stubbs index (top figure), and then introducing it again (bottom figure). It is worth noting that the best results are obtained if all the indices are considered.

The analysis is then extended to other damage scenarios. In Fig. 4 the normalized indices and the agreement bars are shown with reference to the scenario R0-A2 featured by a damage stiffness ratio $D^*_{14}/D_{14} = 0.841$. From the figure on the left (Fig. 4(a)), it emerges that qualified majority-voting highlights possible damage also in element E_{08}, while unanimity-voting excludes this false positive. A 'weak' false positive in element E_{10} would be included without considering also the Kim & Stubbs method. More challenging cases are provided when stiffness reduction is introduced in the element E_{04}. It is worth noting that small damage in element E_{04} (case B1) is not identified whatever reference state is considered (R0, A1 or A2), independently from the voting scheme. If damage is increased to level B2, unanimity-voting correctly identifies damage in both elements E_{04} and E_{14} as also qualified-majority and proportional-voting do (see Fig. 5(a)). However, a false positive in element E_{07} survives. The main difference among the voting schemes lies in the number of 'weak' false positives (macro-index below the threshold), which slightly increases if the voting scheme is relaxed. It is worth to note that adding the Kim & Stubbs index allows us to cancel the weak false positives in Fig. 5(b) (crosses on the cyan boxes).

6. CONCLUSIONS

Ensemble learning applied to curvature-based indices has improved damage localization especially in terms of eliminating false positives. On the other hand, relaxation of the agreement level by changing the voting scheme has not enabled a higher sensitivity to damage. The present results encourage toward the possibility to combine together different methods to increase their overall accuracy.

ACKNOWLEDGEMENTS

The authors acknowledge the support of the Italian Ministry of University and Research (MUR) through the National Recovery and Resilience Plan (PNRR), Sustainable Mobility Center (CNMS), Spoke 3 Waterways, CN00000023 - CUP B43C22000440001.

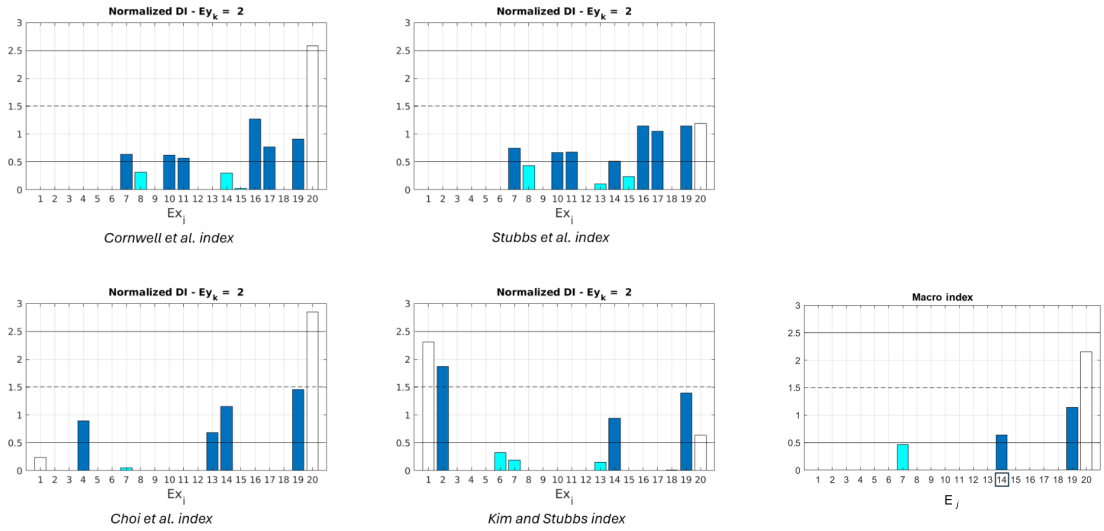

(a) All indices. (b) Macro index evaluation.

Figure 2: Normalized damage indices for scenario R0(intact)-A1(damaged) under SS BCs. Element-weighted stiffness ratio is $\bar{D}^*_{14} = 0.907$.

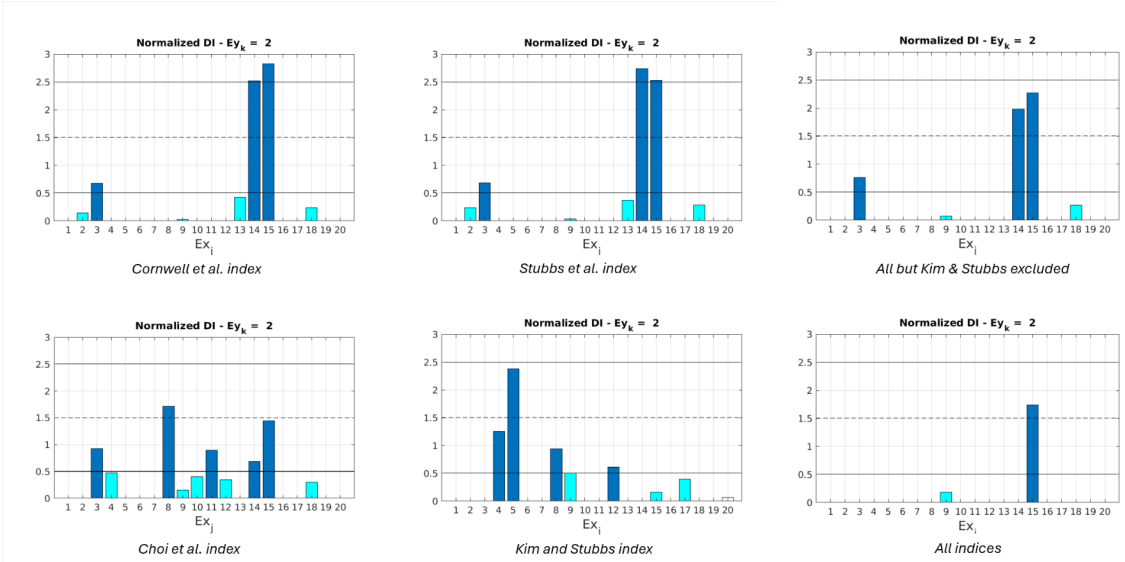

(a) All indices. (b) Macro index evaluation.

Figure 3: Normalized damage indices for scenario A1(intact)-A2(damaged) under SS BCs. Element-weighted stiffness ratio is $\bar{D}^*_{14} = 0.86$.

REFERENCES

[1] Daniele Dessi, Fabio Passacantilli, and Andrea Venturi. Analysis and mitigation of uncertainties in damage identification by modal-curvature based methods. *Journal of Sound and Vibration*, 596: 118769, 2025. ISSN 0022-460X.

[2] A.K. Pandey, M. Biswas, and M.M. Samman. Damage detection from changes in curvature mode shapes. *Journal of Sound and Vibration*, 145(2):321–332, 1991.

[3] W. Fan and P. Qiao. A strain energy-based damage severity correction factor method for damage identification in plate-type structures. *Mechanical Systems and Signal Processing*, 28:210–218, 2012.

[4] Daniele Dessi and Gabriele Camerlengo. Damage identification techniques via modal curvature

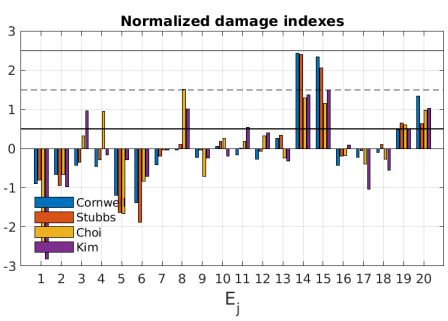

(a) All indices.

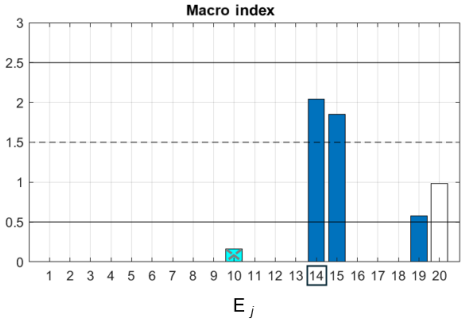

(b) Macro index evaluation.

Figure 4: Normalized damage indices for scenario R0(intact)-A2(damaged) under SS BCs. Element-weighted stiffness ratio is $\bar{D}^*_{14} = 0.841$.

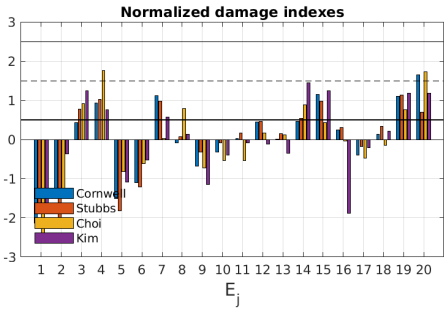

(a) All indices.

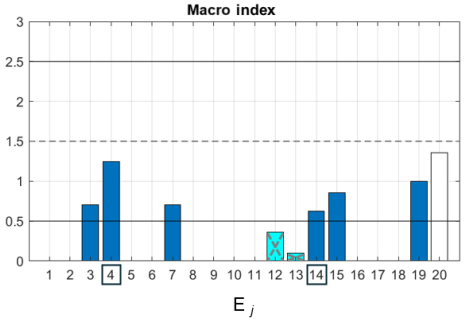

(b) Macro index evaluation.

Figure 5: Normalized damage indices for scenario R0(intact)-B2(damaged) under SS BCs. Element-weighted stiffness ratios are $\bar{D}^*_{14} = 0.841$ and $\bar{D}^*_{04} = 0.841$.

analysis: Overview and comparison. *Mechanical Systems and Signal Processing*, 52-53:181–205, 2015. ISSN 0888-3270.

[5] Daniele Dessi, Fabio Passacantilli, and Andrea Venturi. Hybrid uncertainty analysis of damage indexes based on modal strain energy. In *Proceedings of the 10th International Operational Modal Analysis Conference*, Naples, Italy, 2024.

[6] P. Cornwell, S.W. Doebling, and C.R. Farrar. Application of strain energy damage detection method to plate-like structures. *Journal of Sound and Vibration*, 224(2):359–374, 1999.

[7] N. Stubbs, J-T Kim, and C. R. Farrar. Field verification of a nondestructive damage localization and severity estimation algorithm. In *Proceedings of the 13th International Modal Analysis Conference*, pages 210–218, Nashville, Tennessee, 1995.

[8] J.T. Kim and N. Stubbs. Improved damage identification method based on modal information. *Journal of Sound and Vibration*, 252(2):223–238, 2002.

[9] S. Choi, S. Park, and N. Stubbs. Nondestructive damage detection in structures using changes in compliance. *International Journal of Solids and Structures*, 42(15):4494–4513, 2005.

[10] S. Park, N. Stubbs, R. Bolton, and S. Choi. Improved damage identification method based on modal information. *Computer-Aided Civil and Infrastructure Engineering*, 16:58–70, 2001.

[11] I.D. Mienye and Y. Sun. A survey of ensemble learning: Concepts, algorithms, applications, and prospects. *IEEE Access*, page 3207287, 2022.